Structural and Functional Analyses of the Human-Type Corrinoid Adenosyltransferase (PduO) from Lactobacillus reuteri † , ‡

ARTICLE *in* BIOCHEMISTRY · JANUARY 2008

Impact Factor: 3.02 · DOI: 10.1021/bi701622j · Source: PubMed

4 AUTHORS, INCLUDING:

Ivan Rayment
University of Wisconsin–Madison
233 PUBLICATIONS **14,681** CITATIONS
SEE PROFILE

Jorge C Escalante-Semerena
University of Georgia
175 PUBLICATIONS **5,067** CITATIONS
SEE PROFILE

Structural and Functional Analyses of the Human-Type Corrinoid Adenosyltransferase (PduO) from *Lactobacillus reuteri*[†,‡]

Paola E. Mera,[§] Martin St. Maurice,[||] Ivan Rayment,[||] and Jorge C. Escalante-Semerena*[,§]

Departments of Bacteriology and Biochemistry, University of Wisconsin−Madison, Madison, Wisconsin 53706

Received August 10, 2007; Revised Manuscript Received September 13, 2007

ABSTRACT: ATP:Co(I)rrinoid adenosyltransferase (ACA) catalyzes the conversion of cobalamin to coenzyme B_{12}, an essential cofactor in animal metabolism. Several mutations of conserved residues in the active site of human ACA have been identified in humans with methylmalonic aciduria. However, the catalytic role of these residues remains unclear. To better understand the function of these residues and to determine how the enzyme promotes catalysis, several variants of a human-type ACA from the lactic acid bacterium *Lactobacillus reuteri* (*Lr*PduO) were kinetically and structurally characterized. Kinetic analyses of a series of alternate nucleotides were also performed. Substrate inhibition was observed at subsaturating concentrations of ATP, consistent with an ordered binding scheme where ATP is bound first by the enzyme. Modification or elimination of an active site, inter-subunit salt bridge resulted in a reduced "on" rate for ATP binding, with a less significant disruption in the rate of subsequent catalytic steps. Kinetic and structural data demonstrate that residue Arg^{132} is not involved in orienting ATP in the active site but, rather, it stabilizes the altered substrate in the transition state. Two functional groups of ATP explain the reduced ability of the enzyme to use alternate nucleotides: the amino group at the C-6 position of ATP contributes ~6 kcal/mol of free energy to ground state binding, and the nitrogen at the N-7 position assists in coordinating the magnesium ion in the active site. This study provides new insight into the role of substrate binding determinants and active site residues in the reaction catalyzed by a human-type ACA.

ACAs[1] catalyze the transfer of the adenosyl moiety from ATP to cobalamin (Cbl), generating coenzyme B_{12} (adenosylcobalamin, AdoCbl). The reaction proceeds via the direct nucleophilic attack from the Co(I) ion of the Cbl corrin ring to the C-5′ carbon of ATP, with triphosphate serving as the leaving group (*1*, *2*). AdoCbl is an essential coenzyme in animals, lower eukaryotes, and many prokaryotes, but Cbl is synthesized exclusively by archaea and bacteria (*3*, *4*). The unique and labile organometallic bond between the C-5′ carbon of ATP and cobalt(III) of cobalamin facilitates the unusual chemistry associated with AdoCbl-dependent enzymes (*5*). Enzymes that require AdoCbl catalyze intramolecular rearrangements (*5*−*7*), deaminations (*8*), dehydrations (*9*), reductions (*10*, *11*), and reductive dehalogenations (*12*). There are three types of ACA enzymes. This classification is based on homology of proteins to bona fide corrinoid adenosyltransferases found in the enterobacterium *Salmonella enterica*, namely, CobA, EutT, and PduO (*13*−*15*). CobA, EutT, and PduO are not homologous to each other and are a good example of convergent evolution of proteins that catalyze the same reaction but exhibit different folds.

Animal cells appear to use only PduO-type adenosyltransferases. In these organisms, AdoCbl is required for the function of the mitochondrial methylmalonyl-CoA mutase (MMCM) enzyme. MMCM is part of the pathway that converts propionyl-CoA into succinyl-CoA. MMCM malfunction or defects in other enzymes involved in coenzyme B_{12} synthesis can lead to methylmalonic aciduria and metabolic ketoacidosis (*16*−*18*). These disorders have been associated with developmental retardation and infant mortality (*19*).

Several mutations of the human adenosyltransferase (hATR) have been identified in patients who suffer from methylmalonic aciduria (*16*). In particular, R186W is the most frequently found mutation (~33% of the pathogenic alleles) in patients with methylmalonic aciduria, and has been associated with an early onset of the disease (*20*). Mutations at other positions (e.g., Arg^{190}) have also been associated with this disease. The crystal structures of *Lr*PduO and hATR show that Arg^{190} lies in close proximity to the ATP substrate in the active site (*21*, *22*). Attempts to characterize the role

[†] Work in the Escalante-Semerena lab was supported by NIH Grant R01-GM40313 to J.C.E.-S. Work in the Rayment lab was supported by NIH Grant AR35186. P.E.M. was supported in part by Chemical Biology Interface Training Grant T32 GM008505 (L. L. Kiessling, P.I.) from the National Institute of General Medical Sciences (NIGMS).

[‡] The atomic coordinates and structure factors for R132K and D35N LrPduO have been deposited to the Protein Data Bank, Research Collaboratory for Structural Bioinformatics, Rutgers University, New Brunswick, NJ (http://www.rcsb.org) under the PDB accession numbers 2R6T and 2R6X, respectively.

* Corresponding author: Department of Bacteriology, 1550 Linden Drive, Madison, WI 53706; telephone, 608-262-7379; fax, 608-265-7909; e-mail: escalante@bact.wisc.edu.

[§] Department of Bacteriology.

[||] Department of Biochemistry.

[1] Abbreviations: ACA, ATP:Co(I)rrinoid adenosyltransferase; *Lr*PduO, *Lactobacillus reuteri* PduO; *Se*PduO, *Salmonella enterica* PduO; Cbl, cobalamin; Cbi, cobinamide; AdoCbl, adenosylcobalamin; HOCbl, hydroxycobalamin; MMCM, methylmalonyl-CoA mutase; hATR, human adenosyltransferase; Tris-HCl, tris(hydroxymethyl)-aminomethane hydrochloride; FMN, flavin mononucleotide; MES, morpholinoethanefulfonic acid; NADH, reduced nicotinamide adenine dinucleotide.

10.1021/bi701622j CCC: $37.00
Published on Web 11/08/2007

of these residues in hATR have met with limited success because many mutations have resulted in largely inactive enzyme (*23*, *24*).

Recently the crystal structures of *Lactobacillus reuteri* PduO (*Lr*PduO) and hATR were solved with ATP bound in the active site (*21*, *22*). These structures confirmed that the enzyme is a trimer and that the active site is located at the interface of two adjacent subunits. These structures also revealed that PduO-type ACA enzymes utilize a novel motif to bind ATP. However, the role of individual active site residues in binding and orienting ATP has not been fully established. Here we report the mechanism of binding and orientation of substrates utilized by the PduO-type ACA from *Lactobacillus reuteri*.

EXPERIMENTAL PROCEDURES

Protein Production and Purification. Variants of *L. reuteri* PduO were generated using the QuickChange XL site-directed mutagenesis kit (Stratagene). The pTEV3 plasmid (*21*) carrying the wild-type *Lr* pduO^{+} allele was used as a template for polymerase chain reaction (PCR)-based site directed mutagenesis. To verify the introduction of mutation-(s), plasmids were sequenced at the DNA sequence facility of the University of Wisconsin−Madison. Recombinant *Lr*PduO variants were overexpressed in and purified from *Escherichia coli* strain BL21(DE3) cells transformed with the corresponding pTEV plasmid. The pTEV plasmids encode the *Lr*PduO variants with a rTEV protease-cleavable N-terminal $(His)_6$ tag (*21*).

Crystallization, Data Collection and Structure Determination. In an attempt to cocrystallize the variants with both MgATP and cob(II)alamin, crystals were grown using a reducing system, which included NADH, FMN and a flavodoxin reductase, Fre (*25*). Crystals of tagless *Lr*PduO variants *Lr*PduO^{D35N} and *Lr*PduO^{R132K} were each grown in an anoxic chamber by vapor diffusion at 27 °C by mixing 4 μL of protein solution (15 mg/mL, 30 μg/mL Fre, 50 mM NADH, 10 mM FMN, 10 mM HOCbl, 10 mM MgATP) with 4 μL of reservoir solution (14−16% polyethylene glycol 8000, 100 mM morpholinoethanesulfonic acid (MES) (pH 6), 200 mM KCl). The resulting solution was microseeded after 24 h, resulting in the growth of thin plates (~300 × 300 × 100 μm) within 2−4 days. Crystals were transferred to an anoxic synthetic mother liquor solution (2% glycerol, 11% polyethylene glycol 8000, 100 mM MES (pH 6), 200 mM KCl, 30 μg/mL Fre, 25 mM NADH, 5 mM FMN, 5 mM HOCbl, 10 mM ATP, 12 mM $MgCl_2$) and, in an anoxic chamber, incrementally transferred in five steps to an anoxic cryoprotectant solution (16% ethylene glycol, 13% polyethylene glycol 8000, 100 mM MES (pH 6), 300 mM KCl, 10 mM ATP, 15 mM $MgCl_2$). The crystals were briefly exposed to oxygen (1−2 s) prior to flash freezing in a nitrogen stream at 100 K (Oxford Cryosystems, Oxford, U.K.). The crystals of both variants belong to the space group $P6_3$ with, in each case, two monomers in the asymmetric unit. Datasets were collected at 100 K with a Bruker AXS Platinum 135 CCD detector controlled with the Proteum software suite (Bruker (2004), PROTEUM, Bruker AXS Inc., Madison, WI). The X-ray source was Cu Kα radiation from a Rigaku RU200 X-ray generator equipped with montel optics and operated at 50 kV and 90 mA. These data were processed with SAINT (version V7.06A, Bruker AXS Inc., Madison, WI) and internally scaled with SADABS (version 2005/1, Bruker AXS Inc., Madison, WI). The cumulative intensity distributions for both *Lr*PduO^{D35N} and *Lr*PduO^{R132K} suggested possible merohedral twinning in the crystal lattice and refinement of untreated data resulted in unacceptably high values for R_{cryst} and R_{free}. Consequently, prior to molecular replacement and refinement, both data sets were treated by the program DETWIN (*26*) using the twinning operator (*k*,*h*,−*l*) and a twinning factor of 0.37 for both data sets. The structure was determined by molecular replacement with the program MOLREP (*27*) starting from the model of the wild type *Lr*PduO protein (PDB accession identifier 2NT8). Relevant X-ray data collection and refinement statistics are listed in Table 1, and representative electron density is illustrated in Supplementary Figure 1 (Supporting Information).

Table 1: X-ray Data Collection and Refinement Statistics

	D35N	R132K
space group	$P6_3$	$P6_3$
unit-cell parameters		
(Å)	$a = 65$; $b = 65$; $c = 169$	$a = 65$; $b = 65$; $c = 169$
(deg)	$\alpha = 90$; $\beta = 90$; $\gamma = 120$	$\alpha = 90$; $\beta = 90$; $\gamma = 120$
highest resolution shell (Å)	2.60−2.66	2.61−2.68
resolution range (Å)	2.60−30.0	2.61−30.0
reflections: measured	93 063	76 292
reflections: unique	12 422	12 134
redundancy[a]	7.5 (4.9)	6.3 (4.6)
completeness (%)	99.6 (99.5)	99.6 (97.4)
average I/σ	26.1 (9.3)	18.5 (6.5)
R_{sym} (%)	6.8 (17.7)	8.3 (22.9)
R_{work}	0.173 (0.196)	0.189 (0.192)
R_{free}	0.249 (0.294)	0.259 (0.257)
no. of protein atoms	2785	2874
no. of water molecules	139	96
Wilson *B*-value (Å^2)	29.4	30.3
average B factors (Å^2)		
PduO	31.9	23.8
Mg ATP	29.0	23.4
solvent	34.6	25.3
Ramachandran (%)		
most favored	95.2	95.2
additionally allowed	4.5	4.5
generously allowed	0.0	0.0
disallowed[b]	0.3	0.3
rms deviations		
bond lengths (Å)	0.012	0.012
bond angles (deg)	1.40	1.43

[a] Values in parentheses are for the highest resolution bin (2.60−2.66 Å resolution). [b] Lys^{110} lies in an external loop region of high disorder.

Activity Assays. Corrinoid adenosylation assays were performed at 37 °C using the continuous spectrophotometric method described previously, without modifications (*21*). The adenosylation reaction was initiated by the addition of variant protein to give a final enzyme concentration between 1 and 380 μg/mL, depending on the activity of the variant. AdoCbl formation was monitored at 388 nm (*28*, *29*).

Data Analysis. Kinetic constants were determined by nonlinear regression analysis of initial velocity plots using the program GraphPad Prism 4.0a. Kinetic measurements were taken by holding one substrate at saturation while the other was varied, with the exception of *Lr*PduO^{D35R,R128D}, where very high K_m values precluded measurements at

Scheme 1

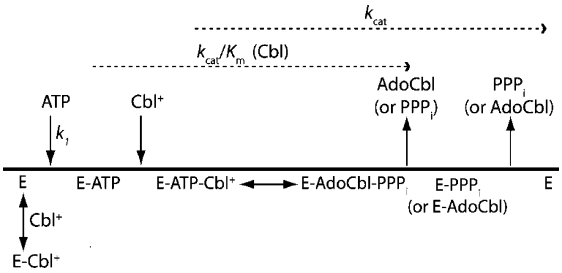

saturation. The kinetic constants of the *Lr*PduO^{D35R,R128D} variant protein with respect to cob(I)alamin and ATP were taken at subsaturating concentrations of Mg-ATP (30 mM) and cob(I)alamin (20 μM). The initial velocity equation for Scheme 1 is given in eq 1 (*30*), where substrate A is ATP and substrate B is cob(I)alamin. This equation is rearranged to eq 2, where the initial velocity is described with respect to substrate B. Substrate inhibition in an ordered bireactant system, therefore, is described in the general form of eq 3 when the concentration of the substrate [A] is kept constant. Initial velocity data were fit to eq 3 using nonlinear regression analysis. All kinetic parameters were determined in duplicate, and average values are reported. The reported errors are standard deviations.

$$v = \frac{V_{max}[A][B]}{K_{ia}K_{mB}\left(1+\frac{[B]}{K_i}\right)+K_{mA}[B]\left(1+\frac{[B]}{K_i}\right)+K_{mB}[A]+[A][B]} \quad (1)$$

$$v = \frac{V_{max}[B]}{K_{mB}\left(1+\frac{K_{iA}}{[A]}\right)+[B]\left(1+\frac{K_{ia}K_{mB}}{K_i[A]}+\frac{K_{mA}}{[A]}\right)+[B]^2\left(\frac{K_{mA}}{K_i[A]}\right)} \quad (2)$$

$$v = \frac{V_{max}[B]}{C_1+[B]C_2+[B]^2C_3} \quad (3)$$

RESULTS

Synthesis of the cobalt−carbon bond in coenzyme B_{12} demands that adenosyltransferase enzymes properly orient cob(I)alamin and ATP to promote nucleophilic attack from the reduced Co^{+1} ion of Cbl to the C-5′ carbon of ATP. The recent reports of the crystal structures of PduO-type ACAs with ATP bound to the active site (*21*, *22*) provide valuable insights into the mechanism by which PduO-type enzymes bind and orient ATP. To further characterize the ATP binding site, and to advance our understanding of the underlying basis for disease in patients suffering from methylmalonic aciduria, we performed detailed kinetic analyses of several enzyme variants and nucleotide substrates.

Order of Binding. The order of substrate binding in ACA enzymes has not been clearly defined. At subsaturating concentrations of ATP (3 μM), substrate inhibition was observed at cobalamin concentrations exceeding 8 μM (Figure 1). However, substrate inhibition was not observed when the concentration of ATP was raised to saturation and the inhibition was reversed by the addition of excess concentrations of ATP (data not shown). Prolonged incubation of *Lr*PduO with cob(I)alamin did not irreversibly inactivate the enzyme. This kinetic profile is consistent with

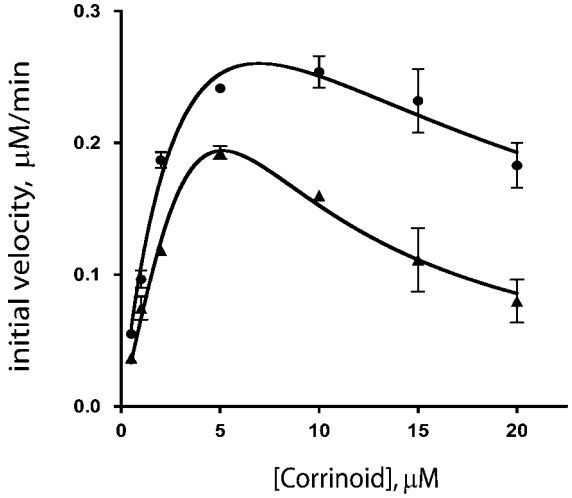

FIGURE 1: Substrate inhibition studies of wild type *Lr*PduO. Plot of initial velocity versus corrinoid concentration. The initial velocities were taken at subsaturating concentrations of MgATP (3μM). Each data point (cobalamin, ●, and cobinamide, ▲) is an average of duplicate assays and errors are reported as standard deviations.

an ordered binding scheme where ATP is bound first, followed by cobalamin (Scheme 1) (*30*). In such a scheme, cob(I)alamin forms a dead-end complex with the enzyme when it binds prior to ATP. *Lr*PduO can also adenosylate cobinamide (Cbi), an incomplete corrinoid lacking the lower 5,6-dimethylbenzimidazole ligand. Cbi also exhibited substrate inhibition at subsaturating concentrations of ATP, but the onset of inhibition occurred at a lower concentration (5 μM). Together, these results strongly support an ordered binding scheme where ATP binding is the essential first step to the enzyme-catalyzed reaction. This is consistent with structural studies, where the Cbl binding pocket includes an N-terminal loop that is ordered only in the presence of bound ATP (*21*, *22*).

Effect of Alternate Nucleotide Substrates on the Rate of Catalysis. PduO-type enzymes utilize a novel structural motif to bind ATP (*21*, *22*) and exhibit reduced specific activities with alternative nucleotides (*15*, *21*, *23*). To further characterize the nucleotide-binding site, we determined detailed kinetic constants for a series of nucleotide analogues (Table 2). Relative to ATP, the purine nucleotides, GTP and ITP, resulted in significantly increased values of K_m (530−13000-fold), with no corresponding decrease in k_{cat}, indicating that binding was principally affected. Conversely, *Lr*PduO exhibited both increased K_m values and reduced turnover numbers with pyrimidine nucleotides (CTP, UTP). When TTP was assayed as a substrate, no detectable product formation was observed. The *Salmonella* housekeeping adenosyltransferase CobA (*Se*CobA) also cannot use TTP as substrate (*31*). Unlike the *Se*CobA enzyme, *Lr*PduO does use 2′-deoxy-ATP as substrate (*32*), but with a 5-fold reduction in the turnover number.

Insights into the Role of Residues Arg^{132}, Arg^{128}, and Asp^{35}. ACA enzymes must bind the nucleotide in an orientation that properly exposes the C-5′ carbon for nucleophilic attack. In both crystal structures of ATP-bound PduO-type enzymes,

Table 2: Kinetic Parameters of Wild-Type *Lr*PduO for Alternate Nucleotides

nucleotide	K_m (μM)	k_{cat} (s^{-1})	k_{cat}/K_m (M^{-1} s^{-1})	$\Delta\Delta G$ (kcal/mol)
ATP	2.2 ± 0.1	$2.6 \pm 0.1 \times 10^{-2}$	$1.2 \pm 0.1 \times 10^{4}$	
GTP	$1.16 \pm 0.04 \times 10^{3}$	$2.1 \pm 0.1 \times 10^{-2}$	$1.8 \pm 0.1 \times 10^{1}$	4.0
ITP	$2.9 \pm 0.8 \times 10^{4}$	$1.9 \pm 0.4 \times 10^{-2}$	$6.5 \pm 2.2 \times 10^{-1}$	6.1
2′-deoxy-ATP	1.60 ± 0.03	$5.1 \pm 0.7 \times 10^{-3}$	$3.3 \pm 0.5 \times 10^{3}$	1.0
CTP	$2.2 \pm 0.2 \times 10^{4}$	$8.6 \pm 0.4 \times 10^{-3}$	$3.8 \pm 0.4 \times 10^{-1}$	6.4
UTP	$4.0 \pm 0.2 \times 10^{4}$	$1.95 \pm 0.02 \times 10^{-3}$	$4.8 \pm 0.3 \times 10^{-2}$	7.7
TTP	ND[a]	ND		

[a] No activity detected.

Table 3: Kinetic Parameters of *Lr*PduO Variants

	ATP			Cbl		
	K_m (μM)	k_{cat} (s^{-1})	k_{cat}/K_m (M^{-1} s^{-1})	K_m (μM)	k_{cat} (s^{-1})	k_{cat}/K_m (M^{-1} s^{-1})
wild type	2.2 ± 0.1	$2.6 \pm 0.1 \times 10^{-2}$	$1.2 \pm 0.1 \times 10^{4}$	0.13 ± 0.01	$2.4 \pm 0.1 \times 10^{-2}$	$1.8 \pm 0.2 \times 10^{5}$
D35N	118 ± 22	$6.1 \pm 0.2 \times 10^{-3}$	$5.2 \pm 1.0 \times 10^{1}$	2.4 ± 0.5	$6.8 \pm 0.4 \times 10^{-3}$	$2.8 \pm 0.6 \times 10^{3}$
R128K	6.2 ± 0.1	$1.12 \pm 0.04 \times 10^{-2}$	$1.8 \pm 0.1 \times 10^{3}$	0.91 ± 0.16	$1.1 \pm 0.1 \times 10^{-2}$	$1.2 \pm 0.2 \times 10^{4}$
R132K	8.4 ± 0.3	$3.3 \pm 0.5 \times 10^{-4}$	$3.9 \pm 0.6 \times 10^{1}$	7.5 ± 0.35	$4.1 \pm 0.05 \times 10^{-4}$	$5.5 \pm 0.3 \times 10^{1}$
S159A	3.8 ± 0.2	$1.69 \pm 0.03 \times 10^{-2}$	$4.5 \pm 0.3 \times 10^{3}$	$2.3 \pm 0.1 \times 10^{-1}$	$1.50 \pm 0.01 \times 10^{-2}$	$6.5 \pm 0.3 \times 10^{4}$
D35N/R128K	410 ± 32	$1.3 \pm 0.1 \times 10^{-2}$	$3.2 \pm 0.3 \times 10^{1}$	3.7 ± 0.6	$1.4 \pm 0.1 \times 10^{-2}$	$3.8 \pm 0.6 \times 10^{3}$
D35E/R128K	96 ± 26	$2.2 \pm 0.1 \times 10^{-3}$	$2.3 \pm 0.6 \times 10^{1}$	2.7 ± 0.9	$2.4 \pm 0.1 \times 10^{-3}$	$9 \pm 3 \times 10^{2}$
D35R/R128D[a]	$9.0 \pm 1.6 \times 10^{3}$	$1.3 \pm 0.2 \times 10^{-4}$	$1.4 \pm 0.3 \times 10^{-2}$	$1.2 \pm 0.3 \times 10^{2}$	$6.5 \pm 0.9 \times 10^{-4}$	5.2 ± 1.5

[a] Kinetic parameters taken at subsaturating concentrations of substrate.

an absolutely conserved Arg residue (Arg^{132} in *Lr*PduO; Arg^{190} in hATR) appears at first sight to orient ATP by hydrogen bonding with the ribose ring oxygen and the bridging oxygen to the α-phosphate. Both Arg → His and Arg → Cys mutations have been identified at this position in patients with methylmalonic aciduria (*20*, *24*). To further investigate the function of residue Arg^{132}, the variant *Lr*PduO^{R132K} was constructed, and its kinetic constants were determined (Table 3). The mutation resulted in a significant reduction (60−80-fold) in the k_{cat} with respect to both substrates, suggesting either that the C-5′ carbon was no longer ideally oriented for attack from the Co^{1+} nucleophile or that the ability of the enzyme to stabilize developing negative charge in the transition state was adversely affected. The k_{cat}/K_m for *Lr*PduO^{R132K} decreased ∼300-fold with respect to ATP and ∼3000-fold with respect to Cbl. The pronounced increase in K_m^{Cbl} suggests a direct interaction between Arg^{132} and Cbl. To probe the relative stringency of the Arg^{132} position, a mutation was directed to the secondary ATP coordination shell of *Lr*PduO. The conserved residue, Ser^{159}, forms a hydrogen bond with Arg^{132} and may, therefore, indirectly influence the substrate orientation. However, the *Lr*PduO^{S159A} variant enzyme exhibited only mild perturbations in the k_{cat} and K_m for both substrates (Table 2).

To gain further insight into the role of Arg^{132} in catalysis, the *Lr*PduO^{R132K} variant was crystallized under anoxic conditions in the presence of MgATP and cob(II)alamin. The X-ray crystal structure was determined to 2.6 Å resolution, revealing two nonphysiologically related monomers in the asymmetric unit (Supplementary Figure 2, Supporting Information). In both monomers, the binding position for MgATP was identical to its position in the wild type enzyme (Figure 2a). No interpretable electron density was observed for the Cbl substrate. The mutated Lys^{132} residue was disordered in one monomer, making no direct contacts with the oxygen atoms of ATP, and was ordered in the second monomer, with its distance to the bridging oxygen of the α-phosphate extended by 1 Å relative to the wild type enzyme. An additional Mg^{2+} ion was observed in the crystal structure of *Lr*PduO^{R132K}, in a position slightly shifted from that observed for a second Mg^{2+} in the human enzyme (*22*).

The mutation R128W of the structurally equivalent residue in hATR (Arg^{186} in hATR) has been identified as the most common mutation in patients with methylmalonic aciduria (*20*). Arg^{128} is conserved in the PduO-type ACAs, and its position in the active site allows for several possible functional roles, including the formation of a critical salt bridge with the conserved Asp^{35} on an adjacent subunit. Several variants were designed with the aim of disrupting the salt bridge between Asp^{35} and Arg^{128}. The kinetic parameters for these variants are presented in Table 3. Size exclusion chromatography confirmed that, like the wild-type enzyme, the variants formed exclusively trimers (data not shown) indicating that this salt bridge does not play a significant role in protein oligomerization. A D35N mutation was introduced with the aim of disrupting the electrostatic interaction with Arg^{128} while preserving the potential to hydrogen bond. Interestingly, while the structure of the wild-type enzyme shows that Asp^{35} does not interact with ATP, the k_{cat}/K_m of *Lr*PduO^{D35N} for ATP decreased 230-fold. Since Asp^{35} interacts exclusively with Arg^{128}, the altered kinetic profile of *Lr*PduO^{D35N} most likely results from a disruption in the bridge formed with Arg^{128}. The *Lr*PduO^{D35N} variant was crystallized under conditions identical to those described for *Lr*PduO^{R128K}, and its structure was determined to 2.6 Å resolution. The electron density maps allowed the position of ATP to be modeled but was uninterpretable for the cob(II)alamin substrate. The structure confirms that the salt bridge between Asp^{35} and Arg^{128} is disrupted by the D35N mutation (Figure 2b). The variant *Lr*PduO^{R128K} exhibited only a small change in its kinetic parameters relative to the wild-type enzyme. In this mutation, the lysine preserves the charge in the active site as well as the potential to form a salt bridge with Asp^{35}. However, a double mutation (D35N/R128K) eliminated this potential interaction and returned the enzyme

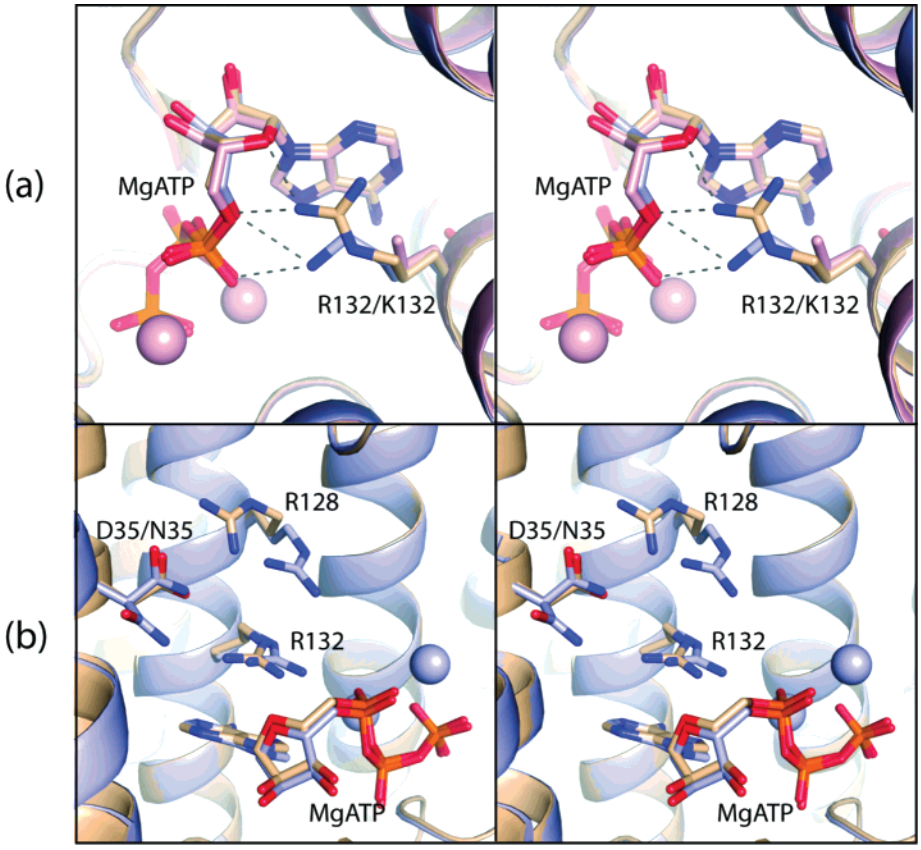

FIGURE 2: Crystal structures of active site variants. (a) Stereoview of a structural overlay of *Lr*PduO^{R132K} monomer A (blue), *Lr*PduO^{R132K} monomer B (pink) and wild-type *Lr*PduO (brown). The rms deviations for alignments with the wild-type enzyme are 0.21 Å, and 0.24 Å for *Lr*PduO^{R132K} monomers A and B, respectively. In monomer A, the ϵ-amino group of Lys^{132} is 3.2 Å removed from the bridging oxygen of the ATP α-phosphate whereas in monomer B, the Lys^{132} side chain is disordered in the electron density map and its position could not be adequately modeled. In all cases, the position and orientation of the ATP substrate is unchanged. (b) Stereoview of a structural overlay of *Lr*PduO^{D35N} monomer A (blue) and wild-type *Lr*PduO in its most commonly observed conformation (brown). The rms deviations for alignments with the wild-type enzyme are 0.17 Å, and 0.24 Å for *Lr*PduO^{D35N} monomers A and B, respectively. The Asn^{35} residue adopts two distinct conformations in the *Lr*PduO^{D35N} variant, but the salt bridge interaction with Arg^{128} has clearly been eliminated.

efficiency to the level observed for the D35N mutation alone. The double mutation D35E/R128K did not restore activity to the level of the R128K mutation alone, indicating that the structural restrictions on the salt bridge are stringent. Finally, reconstitution of this salt bridge was attempted using a reciprocal mutation (D35R/R128D). This variant did not restore wild-type activity and, rather, had such high K_m values that kinetic constants could not be determined at saturation.

DISCUSSION

We analyzed a series of active site variants in the *Lr*PduO enzyme using a combined kinetic and structural approach. Our analysis reveals that the "on" rate for ATP binding is sensitive to the overall integrity of the active site, and that the conserved residue Arg^{132} is not critical to substrate orientation but, rather, is involved in stabilizing developing negative charge in the transition state.

LrPduO Follows an Ordered Substrate Binding Mechanism. The order of substrate binding has not been clearly defined for any type of adenosyltransferase. A detailed kinetic analysis of *Salmonella enterica* PduO showed that catalysis proceeds through a ternary complex (*15*). However, it has not been established whether the reaction follows an ordered or a random mechanism. Both crystal structures of ATP-bound PduO-type enzymes reveal the Cbl binding pocket positioned above a deep ATP binding cleft (*21*, *22*), strongly suggesting that ATP must be bound first by the enzyme. This active site architecture complements spectroscopic analyses which demonstrate that adenosyltransferases generate a requisite four-coordinate cob(II)alamin intermediate only in the presence of ATP (*33*−35). Our observation of substrate inhibition at subsaturating concentrations of ATP is consistent with an ordered binding scheme where ATP binds to the enzyme first and the corrinoid binds second. In such a scheme, ATP binding prevents the formation of a dead-end complex between PduO and cob(I)alamin (Scheme 1).

In an ordered Bi Bi scheme, the k_{cat}/K_m for the first substrate (ATP) is equal to k_1, the "on" rate for ATP binding, and the k_{cat}/K_m for the second substrate (Cbl) represents the composite rate constant for the first committed catalytic step following binding of the second substrate (*30*) (Scheme 1). Thus, mutations in active site residues can be analyzed with respect to the effect of individual mutations on k_{cat} and k_{cat}/K_m values.

The Arg^{128}−Asp^{35} Salt Bridge Influences the Rate for ATP Binding. The most common mutation in human patients suffering from methylmalonic aciduria is structurally equivalent to R128W (*20*). Previous studies have been unsuccessful in characterizing the catalytic role of Arg^{128} because the variants that were generated displayed no enzymatic activity (*23*, *24*). Arg^{128} has several potential roles: it may serve to

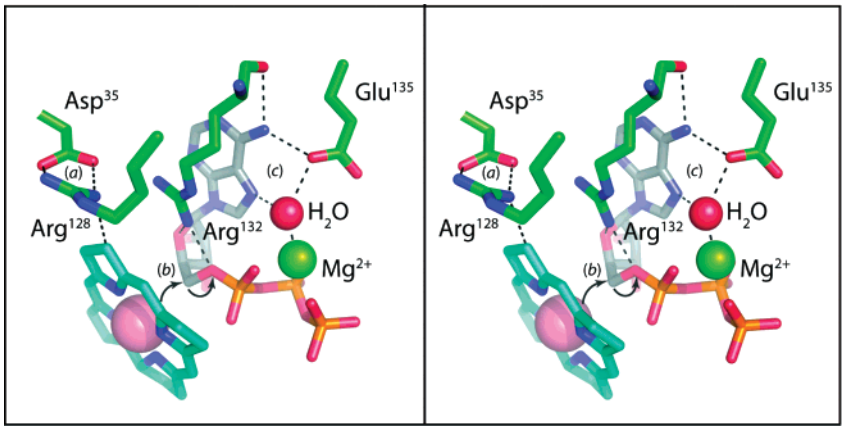

FIGURE 3: Summary of interactions contributing to catalysis in *Lr*PduO. Stereoview of the active site of *Lr*PduO with a schematic representation of the enzyme catalyzed reaction. ATP is shown in gray, and the corrin ring of cob(I)alamin is illustrated in blue. The cob(I)alamin represented in the active site is for illustrative purposes and is not intended to reflect the true conformation of the bound substrate. (*a*) The Arg^{128}—Asp^{35} salt bridge influences the "on" rate for ATP binding, perhaps by reducing the entropic penalty associated with ordering the ATP binding site. Kinetic evidence also favors an interaction between Arg^{128} and Cbl. (*b*) The proximity of Arg^{132} to the α-phosphate of ATP allows for the stabilization of developing negative charge in the transition state. (*c*) The catalytic preference for ATP results from the donation of two hydrogen bonds by the amino group at the C-6 position and the indirect coordination of Mg^{2+} from the N-7 position of the purine ring.

properly orient Arg^{132} for catalysis, it may interact with bound corrinoid, and/or it may serve to maintain the integrity of the active site through an absolutely conserved salt bridge with Asp^{35} of a neighboring subunit. Disruption of the salt bridge leads to a substantial decrease in the rate of ATP binding (230-fold reduction in k_{cat}/K_m for ATP) but has a less significant effect on the transfer step (4-fold reduction in k_{cat} and 60-fold reduction in k_{cat}/K_m for Cbl). The crystal structure of the *Lr*PduO^{D35N} confirms that neither the orientation of ATP nor the conformation of the active site is significantly affected by the loss of this interaction. Nevertheless, the "on" rate for ATP (k_1) is substantially reduced despite the fact that Asp^{35} is 6 Å removed from ATP. The reduced "on" rate for ATP is, therefore, either a direct result of the elimination of the salt bridge or the influence of changing the net charge in the active site. Notably, the R128K mutation maintains both the charge of the active site and the potential to form a salt bridge with Asp^{35} and this variant exhibits only a minor reduction in k_1. Those variants which have both partners of the salt bridge mutated have substantially reduced values of k_1, even in cases where the overall charge of the active site is maintained (e.g., *Lr*PduO$^{D35E/R128K}$).

The binding of ATP to *Lr*PduO is accompanied by the ordering of more than 20 amino acids at the immediate N-terminus of the enzyme, constituting the lower half of the ATP binding site (*21*). A disruption in the Asp^{35}—Arg^{128} salt bridge or an alteration in the charge of the active site will increase the energetic penalty associated with formation of the ATP binding pocket and will reduce the rate of formation of the enzyme—ATP complex. Indeed, studies on the contribution of a salt bridge in the interaction between hen egg white lysozyme and its monoclonal antibody, HyHEL10, have revealed an important entropic role for a salt bridge in suppressing excess conformational changes associated with binding (*36*, *37*). In *Lr*PduO, the Arg^{128}—Asp^{35} salt bridge may provide a similar contribution. The significant reduction observed in k_1 for variants with a deficient salt bridge offers an explanation for why the Arg to Trp mutation leads to inactive enzyme and results in methylmalonic aciduria. The bulky and hydrophobic Trp is incompatible at this location and eliminates this important salt-bridge interaction. If, in addition to the reduction in k_1, the mutation also impairs the binding of Cbl, the enzyme will be rendered even less active.

Arg^{132} Stabilizes the Transition State. The close proximity of Arg^{132} to ATP in the active site suggests an important role for this residue in the reaction (Figure 2a). Structurally equivalent mutations have been identified in humans suffering from methylmalonic aciduria (*20*). Arg^{132} may serve to properly orient the C-5 carbon of ATP for direct nucleophilic attack from the reduced Co^{1+} of Cbl and/or it may assist in stabilizing the negative charge that develops in the transition state. The ~300-fold reduction in the k_{cat}/K_m for ATP confirms that ATP binding is negatively affected by the R132K mutation. The latter also results in a ~3000-fold reduction in the k_{cat}/K_m for Cbl, implying a critical role for Arg^{132} in binding Cbl and promoting adenosyl transfer. The orientation of bound ATP remained unchanged in the crystal structure of *Lr*PduO^{R132K}, even when the side chain of Lys^{132} was found to be disordered. This argues against a role for Arg^{132} in orienting the nucleotide in the active site. The remaining constellation of coordinating residues is sufficient to properly orient ATP. We propose, therefore, that the critical role of Arg^{132} in catalysis is to assist in stabilizing the developing negative charge in the transition state.

The C-6 Amino Group and the N-7 Nitrogen of ATP Facilitate Binding and Catalysis. PduO-type enzymes orient ATP differently from the inverse P-loop used by *Se*CobA (*38*). *Lr*PduO uses 2′-deoxy-ATP as a substrate, whereas *Se*CobA does not, exemplifying this difference in binding modes. Despite these differences, *Lr*PduO and *Se*CobA both have the ability to accept alternate nucleotides as substrates in place of ATP. Two functional groups on ATP help to explain the reduced ability of *Lr*PduO to use alternate nucleotides. Substitution of the hydrogen bond-donating amine of ATP for the hydrogen bond-accepting carbonyl of ITP at the C-6 position resulted in a 13000-fold increase in K_m with no corresponding decrease in k_{cat}. Thus, the amino group at the C-6 position of ATP contributes ~6 kcal/mol

of free energy to ground state binding, equivalent to the energy of donating one to two hydrogen bonds. The K_m increase accompanying ITP binding is about 20-fold greater than that of GTP. This result supports our previous hypothesis that fortuitous interactions can arise between the amino group at the C-2 position of GTP with the backbone carbonyl of Val^{28} (*21*). Unlike the purines (GTP and ITP), pyrimidine substrates resulted in a decrease in k_{cat} in addition to the increased K_m. The nitrogen at the N-7 position of ATP coordinates with a water molecule that serves to chelate the magnesium ion in the active site. Loss of this coordination to water in the pyrimidine substrates may account for their observed decrease in k_{cat}. In addition, the smaller scaffold of the pyrimidine ring alters the fit of these nucleotides in the active site, accounting for both the observed increase in K_m and the decrease in k_{cat}.

The kinetic and structural analysis of *Lr*PduO provides new insight into the role of substrate binding determinants and active site residues in binding ATP and promoting catalysis (summarized in Figure 3). In addition, it further explains the enzyme's preference for ATP and the molecular basis for defects that lead to methylmalonic aciduria.

A more complete description of those residues responsible for binding and catalysis in the human-type adenosyltransferases awaits a high-resolution structure of the enzyme in the presence of both ATP and Cbl.

ACKNOWLEDGMENT

We thank Dr. W. W. Cleland for helpful discussions and critical review of the manuscript.

SUPPORTING INFORMATION AVAILABLE

Supplementary Figure 1 illustrating the representative electron density and Supplementary Figure 2 illustrating the two nonphysiological monomers in the asymmetric unit. This material is available free of charge via the Internet at http://pubs.acs.org.

REFERENCES

1. Huennekens, F. M., Vitols, K. S., Fujii, K., and Jacobsen, D. W. (1982) Biosynthesis of cobalamin coenzymes, in *B12* (Dolphin, D., Ed.) pp 145−168, John Wiley & Sons, Inc., New York.
2. Vitols, E., Walker, G. A., and Huennekens, F. M. (1966) Enzymatic conversion of vitamin B12s to a cobamide coenzyme, α-(5,6-dimethylbenzimidazolyl)deoxy-adenosylcobamide (adenosyl-B12), *J. Biol. Chem. 241*, 1455−1461.
3. Warren, M. J., Raux, E., Schubert, H. L., and Escalante-Semerena, J. C. (2002) The biosynthesis of adenosylcobalamin (vitamin B12), *Nat. Prod. Rep. 19*, 390−412.
4. Roessner, C. A., and Scott, A. I. (2006) Fine-tuning our knowledge of the anaerobic route to cobalamin (vitamin B_{12}), *J. Bacteriol. 188*, 7331−7334.
5. Halpern, J. (1985) Mechanisms of coenzyme B_{12}-dependent rearrangements, *Science 227*, 869−875.
6. Banerjee, R., and Chowdhury, S. (1999) Methylmalonyl-CoA mutase, in *Chemistry and Biochemistry of B12* (Banerjee, R., Ed.) pp 707−729, John Wiley & Sons, Inc., New York.
7. Buckel, W., Bröker, G., Bothe, H., and Pierik, A. (1999) Glutamate mutase and 2-Methylglutarate mutase, in *Chemistry and Biochemistry of B12* (Banerjee, R., Ed.) pp 757−782, John Wiley & Sons, Inc., New York.
8. Bandarian, V., and Reed, G. H. (1999) Ethanolamine ammonia-lyase, in *Chemistry and Biochemistry of B12* (Banerjee, R., Ed.) pp 811−833, John Wiley & Sons, Inc., New York.
9. Toraya, T. (1999) Diol dehydratase and glycerol dehydratase, in *Chemistry and Biochemistry of B12* (Banerjee, R., Ed.) pp 783−809, John Wiley & Sons, Inc., New York.
10. Fontecave, M. (1998) Ribonucleotide reductases and radical reactions, *Cell. Mol. Life Sci. 54*, 684−695.
11. Fontecave, M., and Mulliez, E. (1999) Ribonucleotide Reductases, in *Chemistry and Biochemistry of B12* (Banerjee, R., Ed.) pp 731−756, John Wiley & Sons, Inc., New York.
12. Wohlfarth, G., and Diekert, G. (1999) Reductive dehalogenases, in *Chemistry and Biochemistry of B12* (Banerjee, R., Ed.) pp 871−893, John Wiley & Sons, Inc., New York.
13. Suh, S., and Escalante-Semerena, J. C. (1995) Purification and initial characterization of the ATP:corrinoid adenosyltransferase encoded by the *cobA* gene of *Salmonella typhimurium*, *J. Bacteriol. 177*, 921−925.
14. Buan, N. R., and Escalante-Semerena, J. C. (2006) Purification and initial biochemical characterization of ATP:Cob(I)alamin adenosyltransferase (EutT) enzyme of *Salmonella enterica*, *J. Biol. Chem. 281*, 16971−16977.
15. Johnson, C. L., Buszko, M. L., and Bobik, T. A. (2004) Purification and initial characterization of the *Salmonella enterica* PduO ATP:Cob(I)alamin adenosyltransferase, *J. Bacteriol. 186*, 7881−7887.
16. Dobson, C. M., Wai, T., Leclerc, D., Kadir, H., Narang, M., Lerner-Ellis, J. P., Hudson, T. J., Rosenblatt, D. S., and Gravel, R. A. (2002) Identification of the gene responsible for the cblB complementation group of vitamin B12-dependent methylmalonic aciduria, *Hum. Mol. Genet. 11*, 3361−3369.
17. Fenton, W. A., and Rosenberg, L. E. (1978) Mitochondrial metabolism of hydroxocobalamin: synthesis of adenosylcobalamin by intact rat liver mitochondria, *Arch. Biochem. Biophys. 189*, 441−447.
18. Ciani, F., Donati, M. A., Tulli, G., Poggi, G. M., Pasquini, E., Rosenblatt, D. S., and Zammarchi, E. (2000) Lethal late onset cblB methylmalonic aciduria, *Crit. Care Med. 28*, 2119−2121.
19. Cavicchi, C., Donati, M. A., Funghini, S., la Marca, G., Malvagia, S., Ciani, F., Poggi, G. M., Pasquini, E., Zammarchi, E., and Morrone, A. (2006) Genetic and biochemical approach to early prenatal diagnosis in a family with mut methylmalonic aciduria, *Clin. Genet. 69*, 72−76.
20. Lerner-Ellis, J. P., Gradinger, A. B., Watkins, D., Tirone, J. C., Villeneuve, A., Dobson, C. M., Montpetit, A., Lepage, P., Gravel, R. A., and Rosenblatt, D. S. (2006) Mutation and biochemical analysis of patients belonging to the cblB complementation class of vitamin B12-dependent methylmalonic aciduria, *Mol. Genet. Metab. 87*, 219−225.
21. St Maurice, M., Mera, P. E., Taranto, M. P., Sesma, F., Escalante-Semerena, J. C., and Rayment, I. (2007) Structural characterization of the active site of the PduO-type ATP:Co(I)rrinoid adenosyltransferase from *Lactobacillus reuteri*, *J. Biol. Chem. 282*, 2596−2605.
22. Schubert, H. L., and Hill, C. P. (2006) Structure of ATP-bound human ATP:cobalamin adenosyltransferase, *Biochemistry 45*, 15188−15196.
23. Saridakis, V., Yakunin, A., Xu, X., Anandakumar, P., Pennycooke, M., Gu, J., Cheung, F., Lew, J. M., Sanishvili, R., Joachimiak, A., Arrowsmith, C. H., Christendat, D., and Edwards, A. M. (2004) The structural basis for methylmalonic aciduria. The crystal structure of archaeal ATP:cobalamin adenosyltransferase, *J. Biol. Chem. 279*, 23646−23653.
24. Zhang, J., Dobson, C. M., Wu, X., Lerner-Ellis, J., Rosenblatt, D. S., and Gravel, R. A. (2006) Impact of *cblB* mutations on the function of ATP:cob(I)alamin adenosyltransferase in disorders of vitamin B12 metabolism, *Mol. Genet. Metab. 87*, 315−322.
25. Fonseca, M. V., and Escalante-Semerena, J. C. (2000) Reduction of cob(III)alamin to cob(II)alamin in *Salmonella enterica* Serovar Typhimurium LT2, *J. Bacteriol. 182*, 4304−4309.
26. Taylor, H. O., and Leslie, A. G. W. (1998) A Program to Detwin Merohedrally Twinned Data, *CCP4 Newsl. 35*, 9.
27. Vagin, A., and Teplyakov, A. (1997) MOLREP: an Automated Program for Molecular Replacement, *J. Appl. Crystallogr. 30*, 1022−1025.
28. Buan, N. R., and Escalante-Semerena, J. C. (2005) Computer-assisted docking of flavodoxin with the ATP:Co(I)rrinoid adenosyltransferase (CobA) enzyme reveals residues critical for protein-protein interactions but not for catalysis, *J. Biol.Chem. 280*, 40948−40956.
29. Johnson, C. L., Pechonick, E., Park, S. D., Havemann, G. D., Leal, N. A., and Bobik, T. A. (2001) Functional genomic, biochemical, and genetic characterization of the *Salmonella pduO* gene, an ATP:cob(I)alamin adenosyltransferase gene, *J. Bacteriol. 183*, 1577−1584.

30. Segel, I. H. (1975) *Enzyme Kinetics*, pp 819−822, John Wiley & Sons, New York.
31. Suh, S. J., and Escalante-Semerena, J. C. (1993) Cloning, sequencing and overexpression of *cobA* which encodes ATP: corrinoid adenosyltransferase in *Salmonella typhimurium*, *Gene 129*, 93−97.
32. Fonseca, M. V., Buan, N. R., Horswill, A. R., Rayment, I., and Escalante-Semerena, J. C. (2002) The ATP:co(I)rrinoid adenosyltransferase (CobA) enzyme of *Salmonella enterica* requires the 2′-OH Group of ATP for function and yields inorganic triphosphate as its reaction byproduct, *J. Biol. Chem. 277*, 33127−33131.
33. Stich, T. A., Buan, N. R., and Brunold, T. C. (2004) Spectroscopic and computational studies of Co(2+)corrinoids: spectral and electronic properties of the biologically relevant base-on and base-off forms of Co(2+)cobalamin, *J. Am. Chem. Soc. 126*, 9735−9749.
34. Stich, T. A., Yamanishi, M., Banerjee, R., and Brunold, T. C. (2005) Spectroscopic evidence for the formation of a four-coordinate Co(2+)cobalamin species upon binding to the human ATP:Cobalamin adenosyltransferase, *J. Am. Chem. Soc. 127*, 7660−7661.
35. Stich, T. A., Buan, N. R., Escalante-Semerena, J. C., and Brunold, T. C. (2005) Spectroscopic and computational studies of the ATP: Corrinoid adenosyltransferase (CobA) from *Salmonella enterica*: Insights into the mechanism of adenosylcobalamin biosynthesis, *J. Am. Chem. Soc. 127*, 8710−8719.
36. Shiroishi, M., Yokota, A., Tsumoto, K., Kondo, H., Nishimiya, Y., Horii, K., Matsushima, M., Ogasahara, K., Yutani, K., and Kumagai, I. (2001) Structural evidence for entropic contribution of salt bridge formation to a protein antigen-antibody interaction: the case of hen lysozyme-HyHEL-10 Fv complex, *J. Biol. Chem. 276*, 23042−23050.
37. Tsumoto, K., Ogasahara, K., Ueda, Y., Watanabe, K., Yutani, K., and Kumagai, I. (1996) Role of salt bridge formation in antigen-antibody interaction. Entropic contribution to the complex between hen egg white lysozyme and its monoclonal antibody HyHEL10, *J. Biol. Chem. 271*, 32612−32616.
38. Bauer, C. B., Fonseca, M. V., Holden, H. M., Thoden, J. B., Thompson, T. B., Escalante-Semerena, J. C., and Rayment, I. (2001) Three-dimensional structure of ATP:corrinoid adenosyltransferase from Salmonella typhimurium in its free state, complexed with MgATP, or complexed with hydroxycobalamin and MgATP, *Biochemistry 40*, 361−374.

BI701622J